Genes, Brain and Behavior
Official publication of the International Behavioural and Neural Genetics Society

Genes, Brain and Behavior (2007) **6**: 717–727

Forward genetic screen of mouse reveals dominant missense mutation in the P/Q-type voltage-dependent calcium channel, CACNA1A

G. Xie[†], S. J. Clapcote[†], B. J. Nieman[‡], T. Tallerico[§], Y. Huang[§], I. Vukobradovic[†], S. P. Cordes[†,††], L. R. Osborne[††], J. Rossant[‡,††], J. G. Sled[‡,¶], J. T. Henderson[‡‡] and J. C. Roder*[,†,††]

[†]*Samuel Lunenfeld Research Institute, Mount Sinai Hospital,* [‡]*The Hospital for Sick Children, Mouse Imaging Centre and Research Institute, and* [§]*Department of Medicine,* [¶]*Department of Medical Biophysics,* [††]*Department of Molecular and Medical Genetics, and* [‡‡]*Department of Pharmaceutical Sciences, University of Toronto, Toronto, Canada*

**Corresponding author: J. C. Roder, Samuel Lunefeld Research Institute, Mount Sinai Hospital, 600 University Avenue, Toronto, M5G 1X5, Ontario, Canada. E-mail: roder@mshri.on.ca*

Dominant mutations of the P/Q-type Ca^{2+} channel (CACNA1A) underlie several human neurological disorders, including episodic ataxia type 2, familial hemiplegic migraine 1 (FHM1) and spinocerebellar ataxia 6, but have not been found previously in the mouse. Here we report the first dominant ataxic mouse model of Cacna1a mutation. This *Wobbly* mutant allele of *Cacna1a* was identified in an ethylnitrosourea (ENU) mutagenesis dominant behavioral screen. Heterozygotes exhibit ataxia from 3 weeks of age and have a normal life span. Homozygotes have a righting reflex defect from postnatal day 8 and later develop severe ataxia and die prematurely. Both heterozygotes and homozygotes exhibit cerebellar atrophy with focal reduction of the molecular layer. No obvious loss of Purkinje cells or decrease in size of the granule cell layer was observed. Real-time polymerase chain reaction revealed altered expression levels of *Cacna1g, Calb2* and *Th* in *Wobbly* cerebella, but Cacna1a messenger RNA and protein levels were unchanged. Positional cloning revealed that *Wobbly* mice have a missense mutation leading to an arginine to leucine (R1255L) substitution, resulting in neutralization of a positively charged amino acid in repeat III of voltage sensor segment S4. The dominance of the *Wobbly* mutation more closely resembles patterns of *CACNA1A* mutation in humans than previously described mouse recessive mutants (*tottering, leaner, rolling Nagoya* and *rocker*). Positive-charge neutralization in S4 has also been shown to underlie several cases of human dominant FHM1 with ataxia. The *Wobbly* mutant thus highlights the importance of the voltage sensor and provides a starting point to unravel the neuropathological mechanisms of this disease.

Keywords: Cerebellar ataxia, dominant mutation, ENU, genetic mapping, P/Q type calcium channel

Received 3 November 2006, revised 18 December 2006, accepted for publication 26 December 2006

Voltage-dependent calcium channels (VDCCs) mediate the entry of Ca^{2+} into excitable cells and are also involved in a variety of Ca^{2+}-dependent cellular processes, such as muscle contraction, excitability, neurotransmitter release, gene expression, cell motility, cell division and cell death (Tsien & Tsien 1990; Tsien *et al.* 1991). In mammalian neurons, five major types of VDCCs, designated L, N, R, P/Q and T, have been identified based upon their pharmacological and electrophysiological properties (Bean 1989; Zhang *et al.* 1993). High-threshold VDCCs are multisubunit complexes consisting of α_1, α_2/δ, β, and γ subunits. Channel activity is mainly determined by the pore-forming and voltage-sensitive α_1 subunit, which is encoded by a family of genes (α_{1A} through α_{1I} and α_{1S}) (Birnbaumer *et al.* 1994; Lee *et al.* 1999). The auxiliary subunits α_2/δ, β and γ modulate channel activity (Ahlijanian *et al.* 1990; Campbell *et al.* 1988; Letts *et al.* 1998; Witcher *et al.* 1993). The Ca^{2+} channel α_{1A} subunit gene (*Cacna1a*) encodes the pore-forming protein of P/Q channels and gives rise to P/Q-type calcium currents. *Cacna1a* is highly expressed in the cerebellum, olfactory bulb, cerebral cortex, hippocampus, inferior colliculus and auditory brain stem (Fletcher *et al.* 1996; Tsujimoto *et al.* 2002). The P-type VDCC is predominantly expressed in cerebellar Purkinje cells, whereas the Q-type is a prominent Ca^{2+} current in the cerebellar granule cells (Bourinet *et al.* 1999; Mintz *et al.* 1992; Zhang *et al.* 1993).

Missense mutations in the human *CACNA1A* gene underlie several neurological disorders, including episodic ataxia type 2, familial hemiplegic migraine 1 (FHM1) and spinocerebellar ataxia 6 (SCA6) (Ophoff *et al.* 1996; Yue *et al.* 1997). In mice, *Cacna1a* mutations have been identified in the cerebellar ataxic and dystonic mutants *tottering* (*Cacna1a*^{tg}; *tg*), *leaner* (*Cacna1a*$^{tg\text{-}la}$; *tg-la*), *rolling Nagoya* (*Cacna1a*$^{tg\text{-}rol}$; *tg-rol*) and *rocker* (*Cacna1a*^{rkr}; *rkr*) (Doyle *et al.* 1997; Fletcher *et al.* 1996; Mori *et al.* 2000; Zwingman *et al.* 2001). In contrast to human *CACNA1A* dominant mutations, mice heterozygous for these mutations appear phenotypically normal. Only homozygous mutants exhibit varying degrees of cerebellar ataxia, absence seizures and paroxysmal dyskinesia, ranging from mild

doi: 10.1111/j.1601-183X.2007.00302.x

(*tottering* and *rocker*) to moderate (*rolling Nagoya*) to severe (*leaner*) (Green *et al.* 1962; Meier & MacPike 1971; Nakane 1976; Oda 1973; Zwingman *et al.* 2001). Moreover, heterozygotes for two null mutations of mouse *Cacna1a* (*Cacna1a*^{tm1Hssh} and *Cacna1a*^{tm1Fcr}) also appear phenotypically normal, despite having a 50% reduction in the P/Q current density (Fletcher *et al.* 2001; Jun *et al.* 1999). Homozygous null mutants have severe ataxia and dystonia and often die by the time of weaning. To explore pathophysiological mechanisms underlying the dominantly inherited human CACNA1A mutations, a mouse model that more accurately recapitulates each of the major features of the human CACNA1A mutant diseases might be helpful.

We describe here a novel dominant mutant allele of the *Cacna1a* gene, which we have termed *Wobbly*. Heterozygous mutant (*Cacna1a*$^{Wb/+}$; *Wb*/+) mice exhibit a wide stance, unstable gait and reduced locomotor activity by postnatal days (P) 21–28. *Wb*/+ mice have a normal life span. Homozygous mutant (*Cacna1a*$^{Wb/Wb}$; *Wb*/*Wb*) mice display difficulty in the righting themselves at P8 and are smaller than their *Wb*/+ or wild-type littermates by this age. These animals also display symptoms of dystonia. *Wb*/*Wb* mice survive to adulthood only when maintained under special conditions. Positional cloning and sequencing revealed that *Wobbly* mice carry a novel missense mutation in the *Cacna1a* gene, leading to a R1255L substitution in the highly conserved, positively charged transmembrane segment S4. *Wobbly*, thus, represents the first dominant ataxic mouse model in the allelic series of mouse *Cacna1a* mutations.

Materials and methods

Mice and ENU mutagenesis

Male B6 mice (JAX Research Systems, Bar Harbor, MN, USA) received three intraperitoneal injections of ENU (85 mg/kg), as previously described (Flenniken *et al.* 2005). Ten weeks following the last ethylnitrosourea (ENU) injection, the mutagenized males were bred to untreated female C3H mice (JAX Research Systems). To detect potential mutants, 3733 G1 progeny (C3HB6F1) of this cross were screened at P28 for abnormalities in behavior or appearance using a modified SHIRPA protocol (Flenniken *et al.* 2005). A male mouse exhibiting an unsteady gait, a wide stance of the hindlimbs and a low locomotor activity was discovered and named *Wobbly*. This founder male was bred to C3H females, and the resulting G2 progeny were put through the same behavior and appearance screen as their sire. Mice exhibiting the characteristic unsteady gait of the *Wobbly* founder were classified as 'affected' and further backcrossed to C3H for four generations (G3-G6) to reduce the B6 proportion of the genetic background and facilitate genetic mapping of the mutation.

To investigate the homozygous phenotype of the *Wobbly* mutation, affected G3 mice were intercrossed, resulting in 17 (48.6%) progeny with an unsteady gait at weaning age, nine (25.7%) that were phenotypically normal, and nine (25.7%) with a severe neurological phenotype recognizable from P8. Because this showed that homozygous and heterozygous *Wobbly* mice could be distinguished phenotypically, thus making them useful for genetic mapping, intercrosses were also set up at G4 and G5.

Heterozygous *leaner* mice (B6.Cg-*Os*+/+*Cacna1a*$^{tg\text{-}la}$/J) were obtained from JAX Research Systems. The *leaner* allele was crossed to C3H for two generations to give it the same genetic background as *Wobbly*. The resulting G2 progeny were used for motor behavior and allelic complementarity tests. All experimental procedures were conducted in accordance with the guidelines of the Canadian Council on Animal Care.

Genetic mapping

Genomic DNA was extracted from tail tissue using a standard procedure. To localize the *Wobbly* mutation to a specific chromosomal region, a panel of 100 single-nucleotide polymorphisms (SNPs) between the B6 and C3H parental strains were used to scan the entire genome of 25 G2 *Wobbly* mice (14 affected, 11 normal) at a resolution of ~20 cM. High-throughput SNP genotyping by fluorescence polarization assay (Hsu *et al.* 2001; Kwok 2002) was undertaken using an Analyst HT fluorescence polarization reader (Molecular Devices, Sunnyvale, CA, USA) and ALLELECALLER software (LJL Biosystems, Sunnyvale, CA, USA). After the *Wobbly* mutation had been mapped to a 21.9-Mb interval of Chr 8 between SNP markers ss4328052 (70.4 Mb) and ss4326018 (92.3 Mb), additional SNPs were used to refine the critical interval to 1.7 Mb in a total of 497 G3-G6 mice. For each SNP, a single-base extension (SBE) primer with a melting temperature of 60–80°C and length of 20–30 bases was designed so that its 3′ end annealed adjacent to the polymorphic base pair. Genomic DNA (10 ng) was amplified inside black, hard-shell, 96-well microplates (MJ Research, Waltham, MA, USA) in 5 μl reaction mixtures of 0.5 μl 10× polymerase chain reaction (PCR) *Taq* Gold buffer (Applied Biosystems, Foster City, CA, USA), 0.5 μl 25 mM $MgCl_2$, 0.05 μl 2.5 mM deoxynucleotide triphosphates (dNTPs), 0.2 μl (1.25 μM each) PCR primers and 0.05 μl AmpliTaq Gold DNA polymerase (5 U/μl). Thermocycling conditions on a PTC-0225 DNA Engine Tetrad PCR machine (MJ Research) were as follows: denaturation at 95°C for 12 min, 15 cycles of 95°C for 30 seconds, 66°C for 30 seconds (step down 1°C per cycle) and 72°C for 30 seconds, followed by 35 cycles of 95°C for 30 seconds, 50°C for 30 seconds and 72°C for 30 seconds and a final extension of 72°C for 6 min. For primer and dNTP degradation, 1 μl enzymatic cocktail containing 0.2 μl (1 U/μl) shrimp alkaline phosphatase (SAP; Roche Diagnostics, Laval, QC, Canada), 0.05 μl (10 U/μl) exonuclease I (USB, Cleveland, OH, USA) and 0.1 μl 10× SAP buffer were added to 2.5 μl PCR product and incubated at 37°C for 60 min before the enzymes were heat inactivated at 80°C for 15 min. For the SBE reaction, 6.5 μl AcycloPrimer-FP mixture of 0.025 μl AcycloPol (PerkinElmer Life Science, Woodbridge, ON, Canada), 1 μl 10× reaction buffer, 0.5 μl Acyclo Terminator Mix and 0.25 μl 10 μM SBE primer were added to the enzymatically treated PCR product. Each 10-μl reaction mixture was incubated at 94°C for 2 min, followed by 30 cycles of 94°C for 10 seconds and 55°C for 30 seconds.

Wobbly mutation analysis

Total RNA was isolated from the brains of phenotypically homozygous mutant, heterozygous mutant and normal littermates. First-strand complementary DNA (cDNA) was synthesized by oligo(dT) priming (SuperScript First-Strand Synthesis System; Invitrogen, Burlington, ON, Canada). Reverse transcriptase–polymerase chain reaction (RT-PCR) primers were designed so that eleven 400- to 800-bp fragments covered the entire 6495-bp messenger RNA (mRNA) sequence of mouse Cacna1a (GenBank accession no. U76716). The RT-PCR products were sequenced using an automated sequencer (ABI Prism 377; Applied Biosystems). After a point mutation was discovered in *Cacna1a* exon 27, the following PCR primers were used to confirm the point mutation in genomic DNA from 93 G3-G6 mice (31 phenotypically homozygous mutant, 31 phenotypically heterozygous mutant and 31 normal littermates) using the fluorescence polarization SNP genotyping assay: F: 5′-tgctttgtctcttcccttcc-3′, R: 5′-tctcagtgttgtgtatggagca-3′ and SBE: 5′-ctccgagtcctccgggtgctac-3′.

Northern and Western blotting

For Northern blotting, 20 μg total RNA isolated from whole brain, skeletal muscle and spinal cord of 6-week-old mice were used for blot hybridization in ULTRAhyb hybridization solution (Ambion, Austin, TX, USA) with a ^{32}P-labeled probe (RadPrime DNA labeling system; Invitrogen) consisting of nucleotides 427–1097 of the mouse *Cacna1a* transcript. For Western blotting, 25 μg protein extracted from cerebellum, forebrain, skeletal muscle and spinal cord of 6-week-old mice were subjected to sodium dodecyl sulphate–polyacrylamide gel electrophoresis, transferred to nitrocellulose membranes and incubated

with rabbit anti-$Ca_v2.1$ (Cacna1a) polyclonal antibody (Chemicon, Temecula, CA, USA) in accordance with the vendor's instructions.

Motor behavior tests

To assess the effects of the *Wobbly* mutation on coordinated motor behavior, 8-week-old *Wb*/*Wb*, *Wb*/+, *Wb*/*tg-la*, *tg-la*/+ and +/+ mice were subjected to the following tests of motor performance. **1** Hindlimb extension reflex: Mice were picked up and suspended vertically by the tail at an initial distance of 10 cm from a supportive surface for 3 seconds. The responses of each animal to 10 successive approaches to the support surface were then scored as follows: 0, no extension, clenching of limbs close to body; 1, hindlimb extended on physical contact with the surface, but not upon nose/whisker contact; 2, hindlimb extension upon whisker contact with surface; 3, hindlimb extension immediately prior to whisker contact; 4, pre-emptive, vigorous extension of hindlimbs. Normal mice score 2–3 according to these criteria. **2** Four-limbs grip strength: A mouse grips a graspable surface rod (4-mm diameter), and the force required to relieve this grip is assessed using a dynamometer. Average scores (g) across the best four out of seven trials (30-second inter-trial periods) are reported. **3** Inclined platform: Mice are placed on a wire platform (1- $\times$ 1-cm mesh), which is then inclined to 90°. The time (seconds) it takes a mouse to traverse the entire distance of the platform (24-cm length) with gentle encouragement was then recorded. Mice that fall off the inclined platform are assigned a time of 120 seconds. **4** Beam cross: Mice are placed in the middle of a narrow, graspable runway (3 mm wide, 30 cm long, 28 cm high) and are examined for maneuverability between two stable platforms located at either end. Mice are scored as follows: 1, crosses easily without undue effort, can reverse on 3-mm edge, can reach platform from distance of 15 cm easily; 2, reaches stable platform with substantial difficulty, can reach platform from distances of $<$7 cm, tremor typically evident; 3, extreme difficulty in edge navigation, cannot make progress toward platform, but can maintain grip on edge for a minimum of 8–10 seconds; 4, cannot maintain grip on edge for 8–10 seconds. **5** Rotarod: Performance on a graspable rod (3-cm diameter) is assessed at several (constant) revolution speeds (rpm). Performance was scored as follows: 0 rpm, cannot maintain purchase on stationary rotarod; $<$8 rpm, cannot remain on rotarod at 8 rpm, typically such mice cannot grip rotarod in the inverted position; 15 rpm, maintains purchase on rotarod at 15 rpm for $>$ 5 cycles. Mice are typically examined at each speed for 3 min following a 2-day training period of 15 min each. On the test day, mice are examined for three trials of 3 min each and scored on the basis of their most successful trial.

Magnetic resonance imaging

A cohort of eight *Wb*/*Wb*, four *Wb*/+ and five +/+ littermates were used for *in vivo* magnetic resonance imaging (MRI) scanning at 8 weeks of age. The whole-brain scan was done in parallel to produce 100-μm resolution three-dimensional (3D) data sets (Nieman *et al.* 2005) using a 7-tesla Varian MRI configured for multiple mice. The 3D images were initially aligned to one another by automated linear registration. Analyzing the *Wb*/*Wb* and *Wb*/+ groups separately, deformations were computed using nonlinear registration to bring the individual images in each comparison group into exact alignment. The spatial transformation bringing two brains into alignment was used as a quantitative measure of their difference in shape (Chen *et al.* 2006). The log Jacobians of these transformations were used to compute a Student's *t*-statistic at every voxel.

Immunohistochemistry

Eight-week-old *Wb*/*Wb*, *Wb*/+ and +/+ littermates were lethally anesthetized with tribromoethanol (Avertin, 250 mg/kg). Following a loss of deep tendon responses, the thoracic cavity was opened and mice were perfused through the left ventricle with 10 ml phosphate-buffered saline (PBS; 0.1 M phosphate buffer, pH 7.4; 0.9% NaCl), followed immediately by 4% paraformaldehyde in 0.1 M PBS (PFA) at 25°C. Brains were removed and postfixed overnight in PFA at 4°C. Following infiltration and wax processing, 7-μm paraffin sections were obtained through comparable structural levels for each genotype in either the sagittal or coronal plane. Following dewaxing and the quenching of endogenous peroxidase activity, tissue sections were incubated overnight at 4°C in either rabbit anti-$Ca_v2.1$ (Cacna1a) or rabbit anti-tyrosine hydroxylase (TH) (Chemicon) diluted in primary media (PM; 5% goat serum, 0.2% Tween-20, 0.1 M PBS, pH 7.4). Following rinsing (3 $\times$ 5 min) in PM, sections were incubated for an additional 2 h in the appropriate biotin-labeled secondary antibody (1:200; Vector, Burlingame, CA, USA) at room temperature. After washing in 0.1 M PBS for 3 $\times$ 5 min, sections were incubated with streptavidin-horseradish peroxidase (HRP) for 1 h at room temperature, washed and developed using nickel-enhanced diaminobenzidine (DAB) (Vector).

Analysis of cerebellar molecular layer

Two sets of midsagittal cerebellar sections, spaced 200 μm apart, were prepared from three 8-week-old mice of each genotype (+/+, *Wb*/+, *Wb*/*Wb*). Segments of the cerebellar cortex between lobes V and VI were chosen for analysis. For each slice, linear segments of 600 μm were delineated on lobes V and VI. Thus, for each genotype, average areas of the molecular layer were determined from 36 segments (6 fields $\times$ 2 planes $\times$ 3 mice) of 600 μm in length. For each segment, areas were determined in μm^2 using COMPIX SIMPLE PCI image analysis software. Following an analysis of the normality of the distribution for each data set, genotypes were compared for significance using nonparametric *t*-tests.

Quantitative real-time PCR

Total cerebellar RNA was extracted from six *Wb*/*Wb*, six *Wb*/+ and five +/+ littermates at 8 weeks of age. The cDNA was prepared from 4 μg total RNA per reaction using SuperScript III First-Strand Synthesis System (Invitrogen) according to the manufacturer's instructions. Oligo(dT) was used to prime the cDNA synthesis, and the reaction temperature was 50°C. Real-time PCR was performed in an Mx4000 Multiplex Quantitative PCR System (Stratagene, La Jolla, CA, USA) using Brilliant SYBR Green QPCR Core Reagent kits (Stratagene). Primers were 5′-acagcttcccaaagatgcac-3′ and 5′- acgtccagggagtcagtcct-3′ for *Cacna1g* (GenBank accession no. NM_009783); 5′-gccctcctgaaggatctgta-3′ and 5′-gctcactgcagagcacaatc-3′ for *Calb2* (GenBank accession no. NM_007586); 5′-catagggtaccacccacagg-3′ and 5′-ggttgagaagcagtggagga-3′ for *Th* (GenBank accession no. NM_009377); and 5′-gcatcagaagccgattatcc-3′ and 5′-cagccttctggtactcctca-3′ for *Gusb* (GenBank accession no. NM_010368). DNA standards were PCR amplified, purified and quantified. Standard curves were created by preparing a dilution series of each standard for amplification. Each 25-μl reaction contained 1 μl template, 3.0 mM $MgCl_2$ and 400 nM each primer. The amplification protocol included a 10-min denaturation step, followed by 40 cycles of 95°C for 30 seconds and 59°C for 1 min. The dissociation curve was then generated by stepwise increases in temperature from 55°C to 95°C. Single PCR products were verified by observation of a single peak in the melting curve plot. analysis of variance was used to compare gene expression levels using SPSS 11.0. Homogeneity of variance was tested using the Levene statistic. When variances were found to be equal (*Cacna1g*, $P = 0.815$; *Calb2*, $P = 0.238$), Fisher's least-significant difference post hoc test was used. When Levene's test was significant, indicating unequal variance (*Th*, $P = 0.017$), the Welch *F*-ratio was reported, and a conservative post hoc procedure (Tamhane's T2 test) was used to identify genotype differences.

Results

Phenotypic screening of the Wobbly mutant

The founder *Wobbly* mutant was identified on the basis of its abnormal gait in a behavior and appearance screen of 3733

C3HB6F1 hybrid progeny of ENU mutagenized C57BL/6J (B6) males and untreated C3H/HeJ (C3H) females. The *Wobbly* line was initially maintained by backcrossing to the C3H strain. Thirty of 64 (46.9%) G2 and G3 progeny displayed the abnormal gait of the founder mutant, indicating that the *Wobbly* phenotype is fully penetrant and inherited in an autosomal dominant manner. Heterozygous *Wb*/+ mice were recognizable at P21–28 by their unsteady gait, low body position, splayed hindlimbs and reduced locomotor activity. Heterozygotes had a normal body size and a life span similar to that of wild-type mice (data not shown). Of 187 intercross progeny of *Wb*/+ mutants, 48 (25.7%) mice displayed a severe neurological phenotype at P8, while 93 (49.7%) exhibited an unsteady gait by P21–28, and 46 (24.6%) appeared phenotypically normal. Thus, the unsteady gait of *Wb*/+ mutants was inherited as an autosomal semidominant trait. Homozygous *Wb*/*Wb* mice were easily identifiable at P8 by abnormal righting reflex and smaller size compared with their littermates. By P21, *Wb*/*Wb* mice developed severe ataxia and symptoms of dystonia and often lay on their sides with limbs extended in a stiff posture. Homozygotes died from starvation by P28 unless special provisions were made for access to food and water. Neither *Wb*/+ nor *Wb*/*Wb* mice displayed paroxysmal dyskinesia or motor seizures, nor did abnormal motor behavior progressively worsen with age.

Genetic mapping of the Wobbly mutation

A genome scan of 14 affected and 11 unaffected G2 progeny of the founder *Wobbly* G1 male and C3H females revealed that the characteristic unsteady gait cosegregated with SNP marker ss4319508 at 82.9Mb on chromosome (Chr) 8. An extensive set of SNP markers was used to genotype 497 G3-G6 backcross and intercross progeny to map the mutation to a 1.7-Mb interval between SNP markers ss5034585 (82.7Mb) and ss5109919 (84.4Mb) (Fig. 1). *Cacna1a* was the most appealing candidate gene within this interval.

Wobbly has a missense mutation in Cacna1a

Sequencing of the 6.5-kb coding region of *Cacna1a* cDNA (GenBank accession no. U76716) from *Wobbly* mutants and normal littermates revealed a G-to-T transversion at nucleotide 3764, leading to an arginine (R) 1255 to leucine (L) substitution in *Wb*/*Wb* and *Wb*/+ mice (Fig. 1). This missense mutation was located in exon 27 of the murine *Cacna1a* gene and was not found in genomic DNA from the B6 and C3H parental strains. Segregation analysis of the point mutation, using a fluorescence polarization genotyping assay, revealed coinheritance of the missense mutation and ataxic phenotype in all 31 *Wb*/*Wb* and 31 *Wb*/+ mice tested, while all 31 normal littermates were wild type at the *Wobbly* locus. R1255 is a highly conserved, positively charged amino acid located in the middle of the repeat III S4 transmembrane segment (Fig. 1). The S4 segments of the calcium channel represent the voltage sensor and are characterized by a series of positively charged amino acids at every third position. Northern and Western blot analyses did not detect any differences in brain Cacna1a mRNA and protein expression between *Wb*/*Wb, Wb*/+ and +/+ littermates (Fig. 2).

Wobbly and leaner mutations are allelic

To test for complementarity to a known *Cacna1a* allele such as *leaner*, *Wb*/+ were crossed to *tg-la*/+ mice. As *Wb*/+ mice display a mild ataxic phenotype, while *tg-la*/+ mice are phenotypically normal, it was expected that compound heterozygotes (*Wb*/*tg-la*) would exhibit an ataxic phenotype similar to *Wb*/*Wb* mice if these mutants were allelic to one another. In contrast, if *Wobbly* and *leaner* represented complementary loci, compound heterozygotes should exhibit a phenotype similar to that seen in *Wb*/+ mice. Among 85 progeny of this cross, 21 exhibited a severe dystonic phenotype similar to that seen in *Wb*/*Wb* mice, 20 displayed an ataxic phenotype resembling *Wb*/+ and 44 mice were phenotypically normal. The SNP genotyping of both alleles revealed that all severely affected mice were heterozygous for both the *leaner* and *Wobbly* mutations, whereas all the mildly ataxic mice were heterozygous for the *Wobbly* mutation only. The phenotypically normal mice were either +/+ or *tg-la*/+. This noncomplementation with *leaner* is consistent with *Wobbly* being an allele of *Cacna1a*.

Motor coordination deficits in Wobbly mutant mice

In hindlimb extension reflex tests, *Wb*/*Wb* and *Wb*/*tg-la* mice exhibited an abnormal posture characterized by spasmodic movements and flexion of the hindlimbs. *Wb*/+ mice also had a deficit in this test, while no significant difference was observed between *tg-la*/+ and +/+ littermates (Fig. 3). *Wb*/*Wb* and *Wb*/*tg-la* mice both exhibited significantly reduced grip strength compared with +/+ mice. No significant differences in grip strength were observed between *Wb*/+, *tg-la*/+ and +/+ mice (Fig. 3). In inclined-plane performance, *Wb*/*Wb* and *Wb*/*tg-la* mice performed poorly. *Wb*/+ mice required a significantly longer time than +/+ mice to traverse the inclined platform. Wild-type controls and *tg-la*/+ mice were indistinguishable in this test (Fig. 3). In the narrow-beam cross, a test of fine motor control, both *Wb*/*Wb* and *Wb*/*tg-la* mice were unable to cross the beam toward the platform. *Wb*/+ mice showed some reduced maneuverability compared with wild type and *tg-la*/+ mice (Fig. 3). In rotarod performance, both *Wb*/*Wb* and *Wb*/*tg-la* mice were not able to maintain purchase on a stationary rod. *Wb*/+ mice exhibited substantial difficulty at even low rotation speeds compared with +/+ and *tg-la*/+ mice (Fig. 3). In each of the motor coordination tests, *Wb*/*Wb* exhibited significant deficits compared with *Wb*/+ mice (*P* values in Table 1).

Cerebellar atrophy and reduction of the molecular layer in Wobbly mutant mice

The MRI of the brain and skull in *Wb*/*Wb* and *Wb*/+ mice showed significant cerebellar atrophy compared with +/+ mice. These differences were located primarily in the superior and medial regions of the cerebellum, including lobes III and V (Fig. 4). Segmentation measurement confirmed reduced

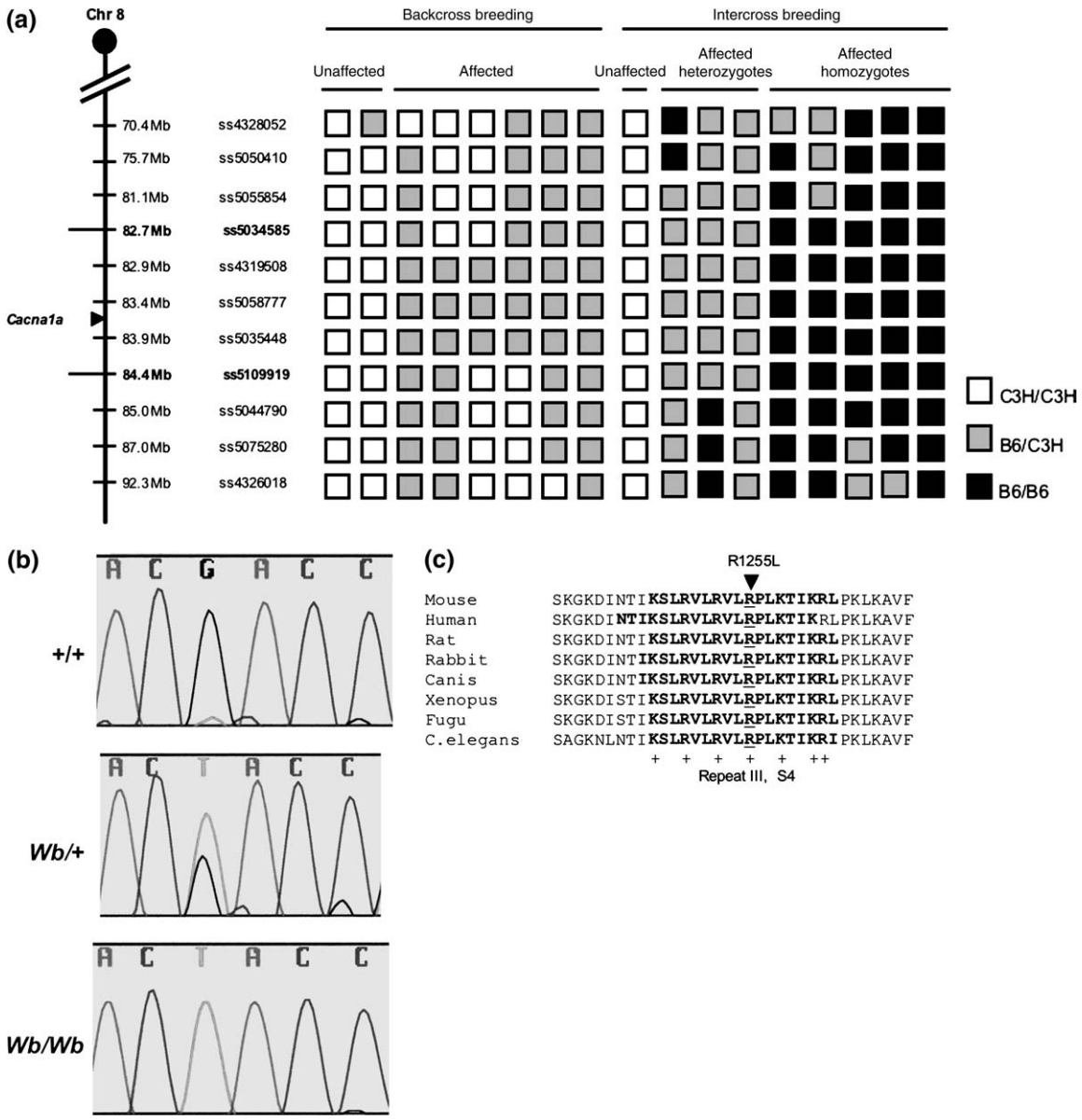

Figure 1: Positional cloning of the *Wobbly* mutation. (a) High-resolution haplotype mapping of *Wobbly* mutation on mouse Chr 8. White squares indicate C3H homozygotes; black squares indicate B6 homozygotes; gray squares indicate B6/C3H heterozygotes. The SNPs defining the minimal interval are shown in bold text. Map positions are in accordance with the public mouse genome assembly (www.ensembl.org/mus_musculus). (b) The cDNA sequencing of mouse *Cacna1a* revealed a G-to-T substitution at nucleotide residue 3764, leading to an arginine (R) to leucine (L) change at residue 1255 in *Wb*/*Wb* and *Wb*/+ mice. (c) Protein sequence alignment of the repeat III voltage sensor S4 segment (bold text) of the P/Q-type Ca^{2+} channel across various species. The *Wobbly* mutation R1255L is positioned at the fourth positively charged amino acid (underlined text).

cerebellum-to-brain volume ratios of 7% and 17% in *Wb*/+ and *Wb*/*Wb*, respectively ($P < 0.01$), compared with +/+ mice. Analysis of the overall cytoarchitecture of +/+, *Wb*/+ and *Wb*/*Wb* adult brain stained with 0.2% cresyl violet revealed no gross cytological abnormalities (data not shown). However, measurements of the width and total area of the molecular layer of the cerebellum revealed significant reduction in *Wb*/+ and *Wb*/*Wb* compared with +/+ mice (Fig. 5). Neither Purkinje cell loss nor a decrease in the size of the granule cell layer was apparent in thionin-stained cerebellar sections from *Wb*/+ and *Wb*/*Wb* mice (Fig. 5). No significant differences were observed in the position or intensity of specific anti-Cacna1a staining within the cerebellum and hippocampus of +/+, *Wb*/+ and *Wb*/*Wb* mice (data not shown).

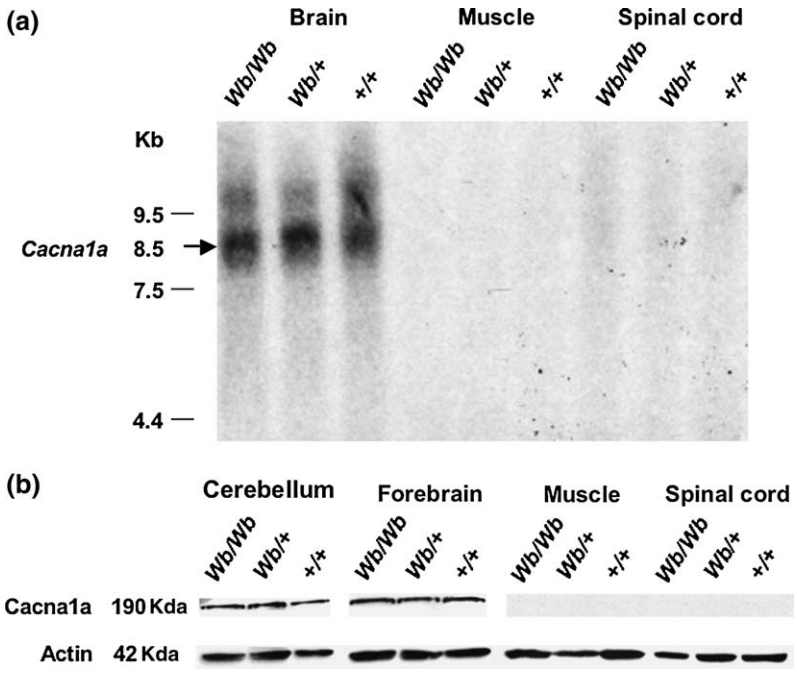

Figure 2: Cacna1a mRNA and protein expression in *Wobbly* mice. Expression of Cacna1a mRNA (a) and protein (b) in the brain, muscle and spinal cord of 6-week-old *Wb*/*Wb*, *Wb*/+ and +/+ littermates. No differences in expression level were observed.

Altered cerebellar mRNA expression of Th, Calb2 and Cacna1g genes in Wobbly mutant mice

Previous studies have shown that the expression of *Th*, *Calb2* and *Cacna1g* genes is altered in the cerebellum of *tg-la*/*tg-la* mutant mice (Hess & Wilson 1991; Nahm *et al.* 2002, 2005). Therefore, we investigated the expression of these genes in the cerebellum of *Wobbly* mice. In *Wobbly* mutant mice, there was a significant effect of genotype on expression levels of *Th*, encoding TH ($F(2,8.67) = 28.116$, $P < 0.0001$), of *Calb2*, encoding calbindin 2 (also known as calretinin) ($F(2,14) = 6.27$, $P = 0.011$) and of *Cacna1g*, encoding the alpha 1G subunit of the T-type VDCCs ($F(2,14) = 8.75$, $P = 0.003$), when normalized by expression of the *Gusb* housekeeping gene (Fig. 6). *Gusb* expression levels were not significantly different between genotypes ($F(2,14) = 1.708$, $P = 0.22$). Real-time PCR standard curve slopes ranged from 3.2 to 3.5, indicating ~93–105% amplification efficiencies. The TH immunostaining localized the increased expression of *Th* within adult *Wb/Wb* cerebellum to a proportion of the Purkinje neurons (data not shown).

Discussion

Cerebellar ataxia was the predominant neurological phenotype observed in *Wobbly* mice. The mild cerebellar ataxia exhibited by *Wb*/+ mice at P21–28 resembled the motor phenotype described for homozygous *tottering* (*tg*/*tg*) mice (Green & Sidman 1962; Nakane 1976). The early onset (P8) of severe motor abnormalities and premature death of unaided *Wb*/*Wb* mice resembled the more severe phenotype described for homozygous *leaner* (*tg-la*/*tg-la*) mice (Meier & MacPike 1971). To address whether heterozygotes for other *Cacna1a* mutant alleles may have previously undetected motor deficits, we used the severe *Cacna1a* mutation *leaner* as a phenotypic comparative control in our battery of motor coordination tests. These tests clearly showed that *Wb*/+ mice have significant motor deficits without loss of muscle strength. In contrast, *tg-la*/+ and +/+ mice were indistinguishable in these tests. *Wb/Wb* and *Wb*/*tg-la* mice showed severe motor coordination deficits and muscle weakness compared with *Wb*/+, *tg-la*/+ and +/+ mice. These results show that the *Wobbly* mutation is semidominant, whereas *leaner* is recessive.

Analysis by MRI revealed significant contraction of the cerebellum in *Wb*/*Wb* and *Wb*/+ mice. Measurements of the width and total area of the molecular layer indicated significant reduction in *Wobbly* mutants, which is similar to the molecular layer-specific decrease in cerebellar volume reported for *tg*/*tg* mice (Isaacs & Abbott 1995). Cerebellar atrophy was more severe in *Wb/Wb* than in the *Wb*/+ mice, which correlated well with the degrees of cerebellar ataxia exhibited by these genotypes. Although motor function in *Wb*/*Wb* mice was as severely affected as that reported for *tg-la*/*tg-la* mice, *Wb*/*Wb* showed no signs of the cerebellar Purkinje cell loss reported for *tg-la*/*tg-la* mice (Herrup & Wilczynski 1982). Cacna1a immunostaining and Northern and Western blot analyses showed no obvious change in *Cacna1a* gene expression within the cerebellum and hippocampus of *Wb/Wb* and *Wb*/+ mice. These findings suggest that the neuropathological alterations of *Wobbly* mutants are the result of post-translational impairment of Ca^{2+} channel activity, rather than progressive apoptotic neuron death in the cerebellum.

The point mutation identified in *Wobbly* mutants is very close to the *rolling Nagoya* (*tg-rol*) mutation in its structural location within the P/Q-type Ca^{2+} channel. Both mutations are located in the voltage sensor of the repeat III S4 segment

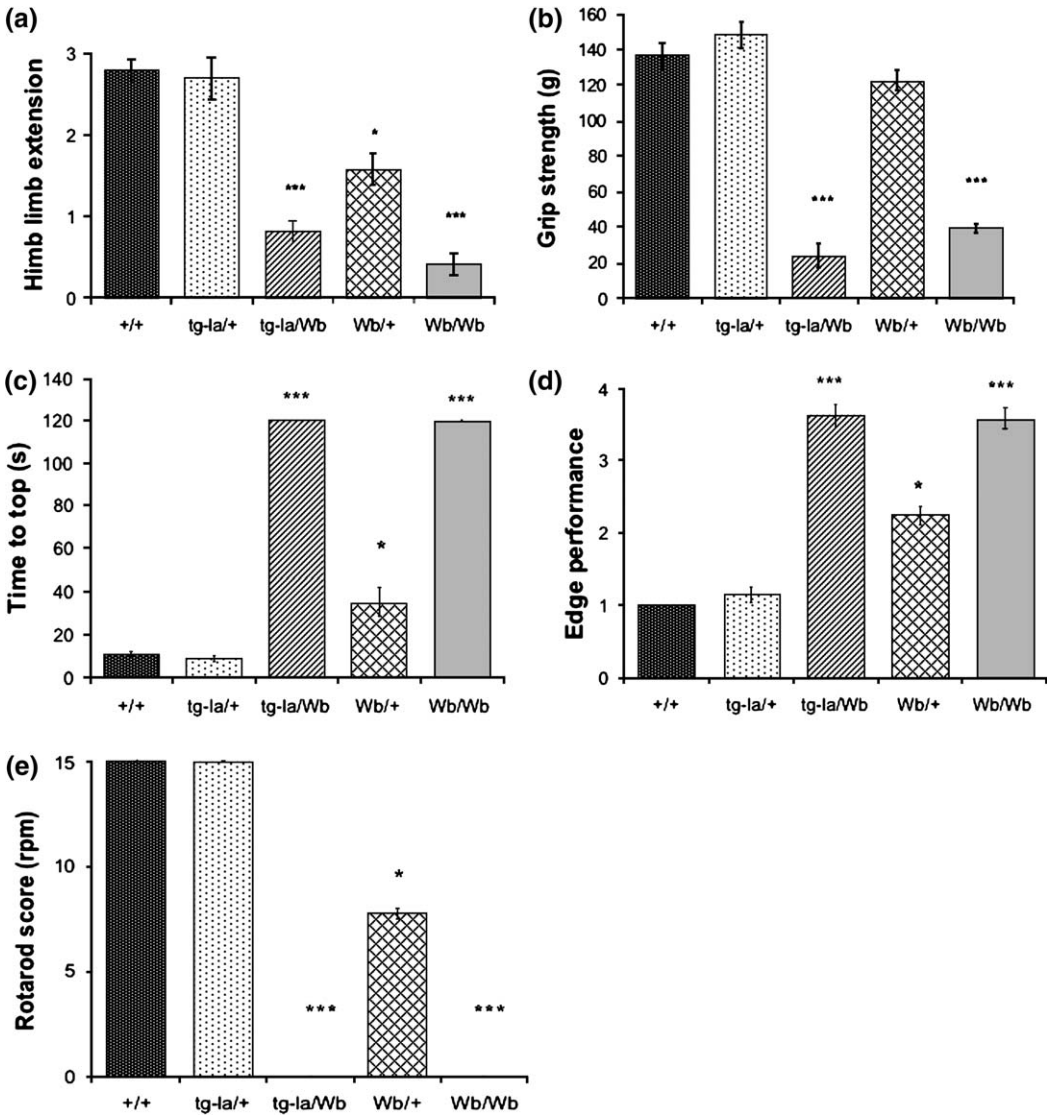

Figure 3: Motor coordination performance of *Wobbly* mice. Adult *Wb*/*Wb* ($n = 12$), *Wb*/+ ($n = 12$), *tg-la*/*Wb* ($n = 11$), *tg-la*/+ ($n = 10$) and +/+ mice ($n = 10$) were examined for (a) hindlimb extension reflex, (b) four-limbs grip strength, (c) 90° climbing platform performance, (d) narrow-beam walking performance, and (e) rotarod performance. *Wb*/+, *Wb*/*Wb* and *tg-la*/*Wb* mice showed significant differences compared with *tg-la*/+ and +/+ mice. $*P < 0.05$; $**P < 0.001$. No significant difference was observed between *tg-la*/+ and +/+ mice.

(Fig. 7). The *Wobbly* mutation leads to the positive charge-neutralizing substitution R1255L, and the *rolling Nagoya* mutation leads to the positive charge-neutralizing change R1262G (Mori *et al.* 2000) (Fig. 1). Leucine (L) and glycine (G) belong to the aliphatic R group, which is nonpolar and hydrophobic. Although these mutations lead to similar ataxic phenotypes in the homozygous state, *Wb/Wb* mice have a more severe cerebellar ataxia with an earlier age of onset than that described for *tg-rol/tg-rol* mice (Nakane 1976; Oda 1973). Notably, *Wobbly* is a semidominant mutation, whereas *rolling Nagoya* is recessive.

Transmembrane S4 segments have been implicated as voltage sensors of different voltage-gated channels (Garcia *et al.* 1997; Liman *et al.* 1991; Pathak *et al.* 2005; Stuhmer *et al.* 1989) and have a characteristic arrangement with a varying number of positively charged amino acids at every third position. It has been shown that the *rolling Nagoya* mutation produces a deficit in the gating properties of the P-type Ca^{2+} channel in Purkinje cells and in transfected BHK6 cells transiently expressing the *rolling Nagoya* mutant P/Q-type channel (Mori *et al.* 2000). Functional and structural studies of the voltage-gated potassium channel *Shaker* (Kv) suggest that the first four positively charged residues (counted from the extracellular side of S4) are the most relevant for voltage sensing (Aggarwal & MacKinnon 1996; Jiang *et al.* 2003; Seoh *et al.* 1996). The *Wobbly* mutation leads to neutralization

Table 1: *P* values in the comparison of genotypes for the motor coordination tests

	Test				
Comparison	Hindlimb extension reflex	Four-limbs grip strength	90° incline	Edge performance	Rotorod (rpm)
Wb/+ vs. +/+	<0.05	>0.05 (NS)	<0.05	<0.05	<0.05
tg-la/+ vs. +/+	>0.05 (NS)	>0.05 (NS)	>0.05 (NS)	>0.05 (NS)	>0.05 (NS)
Wb/+ vs. *tg-la*/+	<0.05	>0.05 (NS)	<0.05	<0.05	<0.05
Wb/*Wb* vs. +/+	<0.0001	<0.0001	<0.0001	<0.0001	<0.0001
tg-la/*Wb* vs. +/+	<0.0001	<0.0001	<0.0001	<0.0001	<0.0001
Wb/*Wb* vs. *tg-la*/*Wb*	>0.05 (NS)	>0.05 (NS)	>0.05 (NS)	>0.05 (NS)	>0.05 (NS)
Wb/+ vs. *Wb*/*Wb*	<0.05	<0.05	<0.05	<0.05	<0.05

P values were obtained using Student's *t*-test or Cochran's *t*-test. NS, not significant.

of the fourth positively charged arginine, and its position complies with the characteristic arrangement of the positively charged amino acids at every third position. However, the *rolling Nagoya* mutation leads to the neutralization of the seventh positively charged arginine, which is an extra positively charged residue in repeat III S4 in a position that deviates from the characteristic arrangement of the positively charged amino acids at every third position (Figs 1,7). Therefore, the *Wobbly* mutation likely alters a functionally more important positively charged residue in S4 than that altered by *rolling Nagoya*, and possibly induces a greater impairment in gate charging of the P/Q-type Ca^{2+} channel than the *rolling Nagoya* mutation does. This could explain why *Wobbly* leads to more severe cerebellar ataxia and is a semidominant mutation.

Real-time PCR analysis revealed significantly enhanced *Th* expression in the cerebellum of both *Wb*/+ and *Wb*/*Wb* mice at 8 weeks of age, which was confirmed by TH immunostaining in adult *Wb*/*Wb* cerebellum. Previous studies have shown increased expression of TH in cerebellar Purkinje cells of adult *tg/tg, tg-la/tg-la* and *tg-rol/tg-rol* mice, while adult heterozygotes for these mutations had no significant change in TH expression (Austin *et al.* 1992; Hess & Wilson 1991; Sawada & Fukui 2001; Sawada *et al.* 2004). The abnormally increased TH in Purkinje cells of *tg-la/tg-la* mice was not enzymatically active and not associated with catecholamine synthesis (Sawada *et al.* 2004). The transcription of *Th* is regulated by Ca^{2+} (Nagamoto-Combs *et al.* 1997) and is facilitated by the activation of N-type or L-type Ca^{2+} channels (Brosenitsch & Katz 2001). In *tg/tg* mice, L-type Ca^{2+} channel expression in

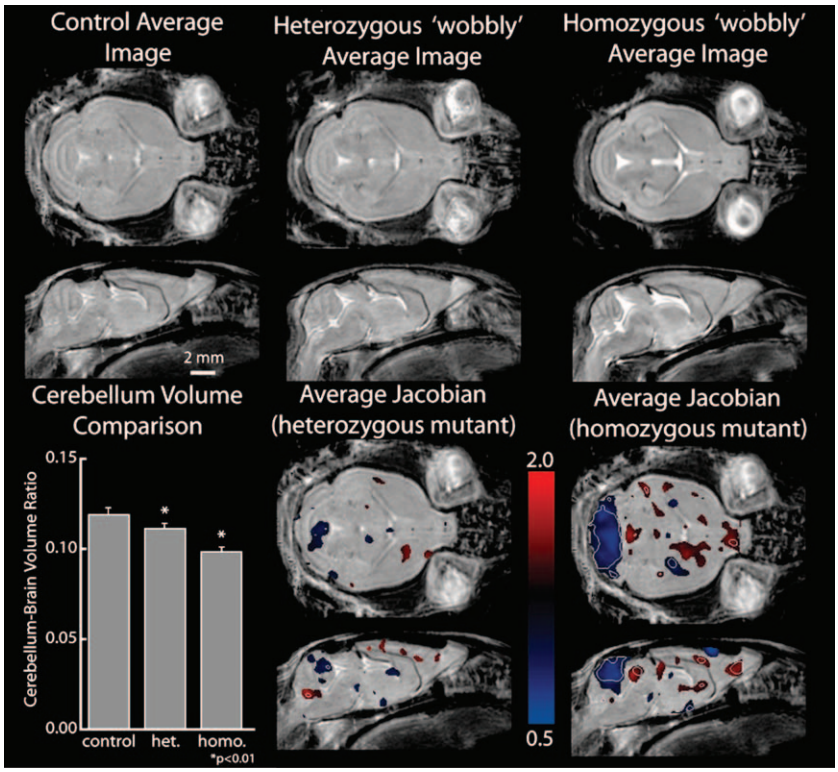

Figure 4: The MRI scans of *Wobbly* mouse brain. Upper panels: Average *Wb*/*Wb* (homozygous 'Wobbly'), *Wb*/+ (heterozygous 'Wobbly') and +/+ (control) images are shown in the horizontal and sagittal orientation. Note the reduced size of the cerebellum in the *Wb*/*Wb* and *Wb*/+ mice. Lower panels: Average Jacobian data are overlaid to indicate regions and severity of abnormalities where $P < 0.05$. White contour lines indicate $P < 0.002$ (5% false discovery rate in *Wb*/*Wb* mice). Bar chart: Differences in cerebellum–brain volume ratios are shown (*$P < 0.01$).

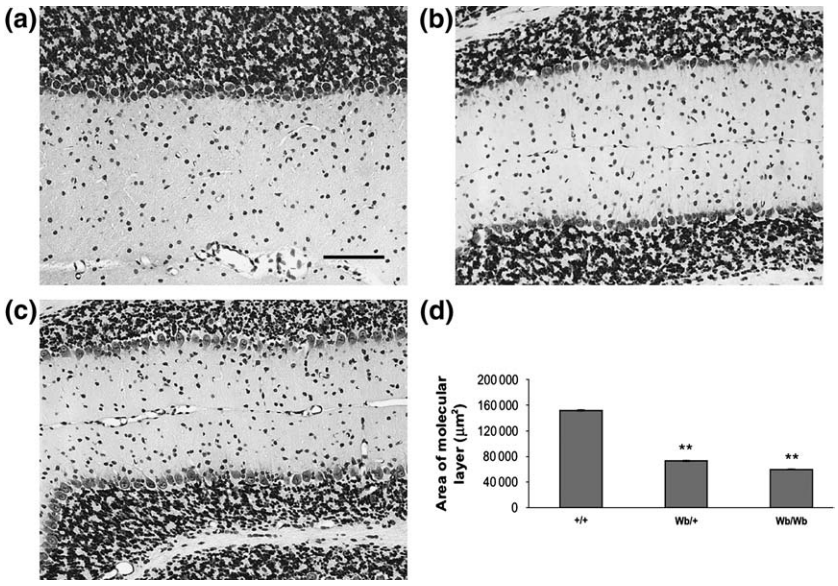

Figure 5: Thionin staining of the cerebellum of (a) +/+, (b) *Wb/+* and (c) *Wb/Wb* mice. The difference in molecular layer area is obvious. Neither Purkinje cell loss nor decrease in the size of the granule cell layers was apparent. (d) Average area (μm^2) of the cerebellar molecular layer of +/+, *Wb*/+ and *Wb*/*Wb* mice calculated from 36 segments of 600 μm in length. Molecular layer area was significantly reduced in *Wb*/+ and *Wb/Wb* mice (**$P < 0.001$). Scale bar indicates 100 μm.

Purkinje cells was increased to compensate for the altered function of the P/Q-type channel (Campbell & Hess 1999), and chronic injections of an L-type Ca^{2+} channel blocker decreased *Th* mRNA expression in the cerebellum (Fureman *et al.* 2003). Thus, the enhanced expression of *Th* in the Purkinje cells of *Wb*/+ mice may reflect neural dysfunction caused by alteration of the intracellular Ca^{2+} concentration that may induce the dominant ataxia of these mice.

Expression of *Calb2* was significantly decreased in the cerebellum of *Wb/Wb* and *Wb*/+ mice. Decreased expression of *Calb2* has also been observed in the cerebellum of *tg-la/tg-la* and *tg/tg* mice (Cicale *et al.* 2002; Nahm *et al.* 2002), while there was no change in *Calb2* expression in *tg*/+ mice (Cicale *et al.* 2002). Calb2 is one component of the extensive Ca^{2+} buffering system that protects cells against an abrupt increase in intracellular Ca^{2+} concentration (Baimbridge *et al.* 1992). *Calb2* null mutants exhibit impaired motor coordination without major disturbance of the cerebellar cytoarchitecture (Schiffmann *et al.* 1999). It has been hypothesized that impaired Ca^{2+} homeostasis in parallel fiber/Purkinje cell synapses could deteriorate cerebellar control of motor coordination, resulting in the cerebellar ataxia of *tg-la/tg-la* and *Calb2* null mice (Cheron *et al.* 2000; Dove *et al.* 2000; Nahm *et al.* 2002). The enhanced expression of *Th* in *Wb*/+ mice could indicate altered intracellular Ca^{2+} concentration in the Purkinje cells, while the decreased expression of *Calb2* in the cerebellum suggests a possible deficit in balancing the altered intracellular Ca^{2+} concentration. Thus, it is tempting to speculate that altered intracellular Ca^{2+} concentration and impaired Ca^{2+} homeostasis may contribute to the motor coordination deficits of *Wb*/+ mice. Consistent with this hypothesis, *tg*/+ mice have unchanged levels of cerebellar TH and Calb2, and exhibit normal neurological behavior (Austin *et al.* 1992; Cicale *et al.* 2002).

Cerebellar expression of *Cacna1g* was significantly decreased in both *Wb*/+ and *Wb/Wb* mice. Cacna1g expression is also significantly decreased in whole cerebellum and granule cells of *tg-la/tg-la* mice (Nahm *et al.* 2005). However, *tg-la/tg-la* Purkinje cells show increased Cacna1g expression. It has been speculated that the paroxysmal dyskinesia exhibited by *tg-la/tg-la* mice is related to this increase in Purkinje cell Cacna1g expression (Nahm *et al.* 2005). If this hypothesis were correct, the lack of paroxysmal dyskinesia in *Wobbly* mice would be predictive of normal Cacna1g expression in *Wobbly* Purkinje cells.

In the human *CACNA1A* gene, seven missense mutations leading to neutralization of the positive charge in voltage sensor S4 segments have been identified (Fig. 7), six of which were identified in FHM1 families with or without cerebellar ataxia (Alonso *et al.* 2004; Ducros *et al.* 2001; Friend *et al.* 1999; Ophoff *et al.* 1996). The seventh mutation

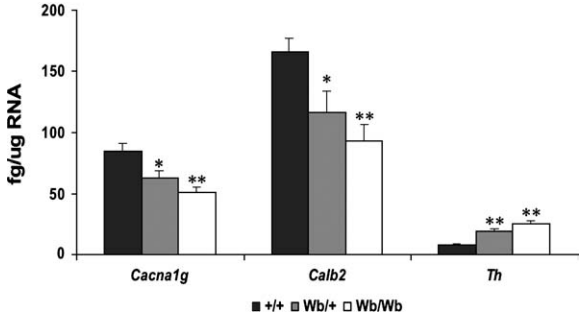

Figure 6: Quantitative real-time PCR analysis of *Cacna1g, Calb2* and *Th* gene expression in the cerebellum of *Wb/Wb, Wb/+* and +/+ mice. *Cacna1g* expression was significantly lower in *Wb*/+ ($P = 0.019$) and *Wb/Wb* ($P = 0.001$) mice than in +/+ mice. *Calb2* expression was significantly lower in *Wb*/+ ($P = 0.033$) and *Wb/Wb* ($P = 0.004$) mice than in +/+ mice. *Th* expression was significantly greater in *Wb*/+ ($P = 0.005$) and *Wb/Wb* ($P = 0.001$) mice than in +/+ mice. Expression levels of *Cacna1g*, *Calb2* and *Th* were not significantly different between *Wb*/+ and *Wb/Wb* mice (*$P < 0.05$).

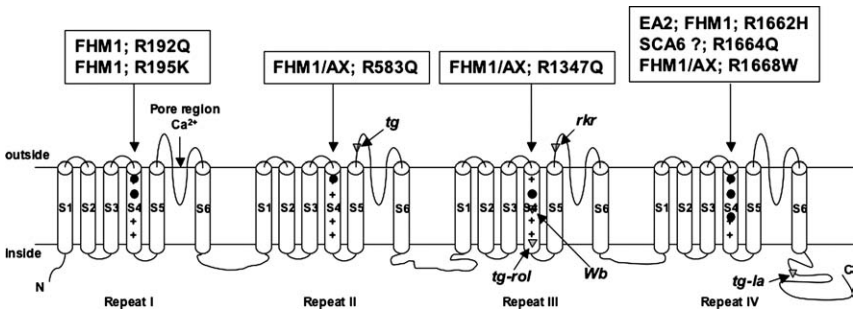

Figure 7: Mouse and human mutations within the alpha 1A subunit of the voltage-dependent P/Q-type calcium channel. The positions of the *Wobbly* (*Wb*), *tottering* (*tg*), *rolling Nagoya* (*tg-rol*), *leaner* (*tg-la*) and *rocker* (*rkr*) mutations of mouse Cacna1a are indicated (gray triangles). The human neurological diseases caused by mutations in the voltage sensor S4 segments of human CACNA1A are named (boxes, top). The positions of the human mutations (closed circles) are according to GenBank accession no. X99897. FHM1/AX: FHM1 with cerebellar ataxia.

was associated with an unconfirmed diagnosis of SCA6 in a 3-year-old patient, in which migraine could not be excluded because of the patient's young age (Tonelli *et al.* 2006). A knockin mouse model carrying the human FHM1 R192Q mutation showed a gain-of-function effect on neuronal Ca^{2+} current, enhanced neurotransmitter release and lowered threshold for cortical spreading depression (van den Maagdenberg *et al.* 2004). However, the R192Q mutant mouse appeared phenotypically normal and had no cytoarchitectural abnormalities in the brain (van den Maagdenberg *et al.* 2004). In FHM1 patients with ataxia who have been examined by MRI, cerebellar atrophy was detected (Alonso *et al.* 2004; Ducros *et al.* 2001; Friend *et al.* 1999). Interestingly, the mouse *Wobbly* mutation leading to neutralization of the fourth positively charged amino acid in repeat III S4 is remarkably similar to a human missense mutation leading to neutralization of the second positively charged amino acid (R1347Q) in repeat III S4 in a Portuguese FHM1 family with cerebellar ataxia and atrophy (Figs 1,7) (Alonso *et al.* 2004). The position of the *Wobbly* missense mutation within S4, the phenotype of cerebellar ataxia and atrophy and particularly the dominant inheritance of the *Wobbly* mutant thus make it a better mouse model of the human condition than the existing mouse *Cacna1a* mutants.

References

Aggarwal, S.K. & MacKinnon, R. (1996) Contribution of the S4 segment to gating charge in the Shaker K^+ channel. *Neuron* **16**, 1169–1177.

Ahlijanian, M.K., Westenbroek, R.E. & Catterall, W.A. (1990) Subunit structure and localization of dihydropyridine-sensitive calcium channels in mammalian brain, spinal cord, and retina. *Neuron* **4**, 819–832.

Alonso, I., Barros, J., Tuna, A., Seixas, A., Coutinho, P., Sequeiros, J. & Silveira, I. (2004) A novel R1347Q mutation in the predicted voltage sensor segment of the P/Q-type calcium-channel alpha-subunit in a family with progressive cerebellar ataxia and hemiplegic migraine. *Clin Genet* **65**, 70–72.

Austin, M.C., Schultzberg, M., Abbott, L.C., Montpied, P., Evers, J.R., Paul, S.M. & Crawley, J.N. (1992) Expression of tyrosine hydroxylase in cerebellar Purkinje neurons of the mutant tottering and leaner mouse. *Mol Brain Res* **15**, 227–240.

Baimbridge, K.G., Celio, M.R. & Rogers, J.H. (1992) Calcium-binding proteins in the nervous system. *Trends Neurosci* **15**, 303–308.

Bean, B.P. (1989) Classes of calcium channels in vertebrate cells. *Annu Rev Physiol* **51**, 367–384.

Birnbaumer, L., Campbell, K.P., Catterall, W.A., Harpold, M.M., Hofmann, F., Horne, W.A., Mori, Y., Schwartz, A., Snutch, T.P. & Tanabe, T. (1994) The naming of voltage-gated calcium channels. *Neuron* **13**, 505–506.

Bourinet, E., Soong, T.W., Sutton, K., Slaymaker, S., Mathews, E., Monteil, A., Zamponi, G.W., Nargeot, J. & Snutch, T.P. (1999) Splicing of alpha 1A subunit gene generates phenotypic variants of P- and Q-type calcium channels. *Nat Neurosci* **2**, 407–415.

Brosenitsch, T.A. & Katz, D.M. (2001) Physiological patterns of electrical stimulation can induce neuronal gene expression by activating N-type calcium channels. *J Neurosci* **21**, 2571–2579.

Campbell, D.B. & Hess, E.J. (1999) L-type calcium channels contribute to the tottering mouse dystonic episodes. *Mol Pharmacol* **55**, 23–31.

Campbell, K.P., Leung, A.T. & Sharp, A.H. (1988) The biochemistry and molecular biology of the dihydropyridine-sensitive calcium channel. *Trends Neurosci* **11**, 425–430.

Chen, X.J., Kovacevic, N., Lobaugh, N.J., Sled, J.G., Henkelman, R.M. & Henderson, J.T. (2006) Neuroanatomical differences between mouse strains as shown by high-resolution 3D MRI. *Neuroimage* **29**, 99–105.

Cheron, G., Schurmans, S., Lohof, A., d'Alcantara, P., Meyer, M., Draye, J.P., Parmentier, M. & Schiffmann, S.N. (2000) Electrophysiological behavior of Purkinje cells and motor coordination in calretinin knock-out mice. *Prog Brain Res* **124**, 299–308.

Cicale, M., Ambesi-Impiombato, A., Cimini, V., Fiore, G., Muscettola, G., Abbott, L.C. & de Bartolomeis, A. (2002) Decreased gene expression of calretinin and ryanodine receptor type 1 in tottering mice. *Brain Res Bull* **59**, 53–58.

Dove, L.S., Nahm, S.S., Murchison, D., Abbott, L.C. & Griffith, W.H. (2000) Altered calcium homeostasis in cerebellar Purkinje cells of leaner mutant mice. *J Neurophysiol* **84**, 513–524.

Doyle, J., Ren, X., Lennon, G. & Stubbs, L. (1997) Mutations in the Cacnl1a4 calcium channel gene are associated with seizures, cerebellar degeneration, and ataxia in tottering and leaner mutant mice. *Mamm Genome* **8**, 113–120.

Ducros, A., Denier, C., Joutel, A., Cecillon, M., Lescoat, C., Vahedi, K., Darcel, F., Vicaut, E., Bousser, M.G. & Tournier-Lasserve, E. (2001) The clinical spectrum of familial hemiplegic migraine associated with mutations in a neuronal calcium channel. *N Engl J Med* **345**, 17–24.

Flenniken, A.M., Osborne, L.R., Anderson, N. *et al.* (2005) A Gja1 missense mutation in a mouse model of oculodentodigital dysplasia. *Development* **132**, 4375–4386.

Fletcher, C.F., Lutz, C.M., O'Sullivan, T.N., Shaughnessy, J.D., Hawkes, R., Frankel, W.N., Copeland, N.G. & Jenkins, N.A. (1996) Absence epilepsy in tottering mutant mice is associated with calcium channel defects. *Cell* **87**, 607–617.

Fletcher, C.F., Tottene, A., Lennon, V.A., Wilson, S.M., Dubel, S.J., Paylor, R., Hosford, D.A., Tessarollo, L., McEnery, M.W.,

Pietrobon, D., Cope land, N.G. & Jenkins, N.A. (2001) Dystonia and cerebellar atrophy in Cacna1a null mice lacking P/Q calcium channel activity. *FASEB J* **15**, 1288–1290.
Friend, K.L., Crimmins, D., Phan, T.G., Sue, C.M., Colley, A., Fung, V.S., Morris, J.G., Sutherland, G.R. & Richards, R.I. (1999) Detection of a novel missense mutation and second recurrent mutation in the CACNA1A gene in individuals with EA-2 and FHM. *Hum Genet* **105**, 261–265.
Fureman, B.E., Campbell, D.B. & Hess, E.J. (2003) Regulation of tyrosine hydroxylase expression in tottering mouse Purkinje cells. *Neurotox Res* **5**, 521–528.
Garcia, J., Nakai, J., Imoto, K. & Beam, K.G. (1997) Role of S4 segments and the leucine heptad motif in the activation of an L-type calcium channel. *Biophys J* **72**, 2515–2523.
Green, M.C. & Sidman, R.L. (1962) Tottering – a neuromusclar mutation in the mouse. And its linkage with oligosyndacylism. *J Hered* **53**, 233–237.
Herrup, K. & Wilczynski, S.L. (1982) Cerebellar cell degeneration in the leaner mutant mouse. *Neuroscience* **7**, 2185–2196.
Hess, E.J. & Wilson, M.C. (1991) Tottering and leaner mutations perturb transient developmental expression of tyrosine hydroxylase in embryologically distinct Purkinje cells. *Neuron* **6**, 123–132.
Hsu, T.M., Chen, X., Duan, S., Miller, R.D. & Kwok, P.Y. (2001) Universal SNP genotyping assay with fluorescence polarization detection. *Biotechniques* **31**, 560–568.
Isaacs, K.R. & Abbott, L.C. (1995) Cerebellar volume decreases in the tottering mouse are specific to the molecular layer. *Brain Res Bull* **36**, 309–314.
Jiang, Y., Ruta, V., Chen, J., Lee, A. & MacKinnon, R. (2003) The principle of gating charge movement in a voltage-dependent K^+ channel. *Nature* **423**, 42–48.
Jun, K., Piedras-Renteria, E.S., Smith, S.M., Wheeler, D.B., Lee, S.B., Lee, T.G., Chin, H., Adams, M.E., Scheller, R.H., Tsien, R.W. & Shin, H.S. (1999) Ablation of P/Q-type Ca^{2+} channel currents, altered synaptic transmission, and progressive ataxia in mice lacking the α1A-subunit. *Proc Natl Acad Sci USA* **96**, 15245–15250.
Kwok, P.Y. (2002) SNP genotyping with fluorescence polarization detection. *Hum Mutat* **19**, 315–323.
Lee, J.H., Daud, A.N., Cribbs, L.L., Lacerda, A.E., Pereverzev, A., Klockner, U., Schneider, T. & Perez-Reyes, E. (1999) Cloning and expression of a novel member of the low voltage-activated T-type calcium channel family. *J Neurosci* **19**, 1912–1921.
Letts, V.A., Felix, R., Biddlecome, G.H., Arikkath, J., Mahaffey, C.L., Valenzuela, A., Bartlett, F.S., Mori, Y., Campbell, K.P. & Frankel, W.N. (1998) The mouse stargazer gene encodes a neuronal Ca^{2+}-channel gamma subunit. *Nat Genet* **19**, 340–347.
Liman, E.R., Hess, P., Weaver, F. & Koren, G. (1991) Voltage-sensing residues in the S4 region of a mammalian K^+ channel. *Nature* **353**, 752–756.
van den Maagdenberg, A.M., Pietrobon, D., Pizzorusso, T., Kaja, S., Broos, L.A., Cesetti, T., van de Ven, R.C., Tottene, A., van der Kaa, J., Plomp, J.J., Frants, R.R. & Ferrari, M.D. (2004) A Cacna1a knockin migraine mouse model with increased susceptibility to cortical spreading depression. *Neuron* **41**, 701–710.
Meier, H. & MacPike, A.D. (1971) Three syndromes produced by two mutant genes in the mouse. Clinical, pathological, and ultrastructural bases of tottering, leaner, and heterozygous mice. *J Hered* **62**, 297–302.
Mintz, I.M., Adams, M.E. & Bean B.P. (1992) P-type calcium channels in rat central and peripheral neurons. *Neuron* **9**, 85–95.
Mori, Y., Wakamori, M., Oda, S., Fletcher, C.F., Sekiguchi, N., Mori, E., Copeland, N.G., Jenkins, N.A., Matsushita, K., Matsuyama, Z. & Imoto, K. (2000) Reduced voltage sensitivity of activation of P/Q-type Ca^{2+} channels is associated with the ataxic mouse mutation rolling Nagoya (tg^{rol}). *J Neurosci* **20**, 5654–5662.
Nagamoto-Combs, K., Piech, K.M., Best, J.A., Sun, B. & Tank, A.W. (1997) Tyrosine hydroxylase gene promoter activity is regulated by both cyclic AMP-responsive element and AP1 sites following calcium influx. *J Biol Chem* **272**, 6051–6058.
Nahm, S.S., Tomlinson, D.J. & Abbott, L.C. (2002) Decreased calretinin expression in cerebellar granule cells in the leaner mouse. *J Neurobiol* **51**, 313–322.
Nahm, S.S., Jung, K.Y., Enger, M.K., Griffith, W.H. & Abbott, L.C. (2005) Differential expression of T-type calcium channels in P/Q-type calcium channel mutant mice with ataxia and absence epilepsy. *J Neurobiol* **62**, 352–360.
Nakane, K. (1976) Postnatal development of brain with congential ataxia, rolling (rol) and tottering (tg). *Teratology* **14**, 248–249.
Nieman, B.J., Bock, N.A., Bishop, J., Sled, J.G., Chen, X.J. & Henkelman, R.M. (2005) Fast spin-echo for multiple mouse magnetic resonance phenotyping. *Magn Reson Med* **54**, 532–537.
Oda, S. (1973) The observation of rolling mouse Nagoya (rol), a new neurological mutant, and its maintenance. *Exp Anim* **22**, 281–288.
Ophoff, R.A., Terwindt, G.M., Vergouwe, M.N., van Eijk, R., Oefner, P.J., Hoffman, S.M., Lamerdin, J.E., Mohrenweiser, H.W., Bulman, D.E., Ferrari, M., Haan, J., Lindhout, D., van Ommen, G.J., Hofker, M.H., Ferrari, M.D. & Frants, R.R. (1996) Familial hemiplegic migraine and episodic ataxia type-2 are caused by mutations in the Ca^{2+} channel gene CACNL1A4. *Cell* **87**, 543–552.
Pathak, M., Kurtz, L., Tombola, F. & Isacoff, E. (2005) The cooperative voltage sensor motion that gates a potassium channel. *J Gen Physiol* **125**, 57–69.
Sawada, K. & Fukui, Y. (2001) Expression of tyrosine hydroxylase in cerebellar Purkinje cells of ataxic mutant mice: its relation to the onset and/or development of ataxia. *J Med Invest* **48**, 5–10.
Sawada, K., Ando, M., Sakata-Haga, H., Sun, X.Z., Jeong, Y.G., Hisano, S., Takeda, N. & Fukui, Y. (2004) Abnormal expression of tyrosine hydroxylase not accompanied by phosphorylation at serine 40 in cerebellar Purkinje cells of ataxic mutant mice, rolling mouse Nagoya and dilute-lethal. *Congenit Anom* **44**, 46–50. Erratum in: *Congenit Anom* 44, 178–179.
Schiffmann, S.N., Cheron, G., Lohof, A., d'Alcantara, P., Meyer, M., Parmentier, M. & Schurmans, S. (1999) Impaired motor coordination and Purkinje cell excitability in mice lacking calretinin. *Proc Natl Acad Sci USA* **96**, 5257–5262.
Seoh, S.A., Sigg, D., Papazian, D.M. & Bezanilla, F. (1996) Voltage–sensing residues in the S2 and S4 segments of the Shaker K^+ channel. *Neuron* **16**, 1159–1167.
Stuhmer, W., Conti, F., Suzuki, H., Wang, X.D., Noda, M., Yahagi, N., Kubo, H. & Numa, S. (1989) Structural parts involved in activation and inactivation of the sodium channel. *Nature* **339**, 597–603.
Tonelli, A., D'Angelo, M.G., Salati, R., Villa, L., Germinasi, C., Frattini, T., Meola, G., Turconi, A.C., Bresolin, N. & Bassi, M.T. (2006) Early onset, non fluctuating spinocerebellar ataxia and a novel missense mutation in CACNA1A gene. *J Neurol Sci* **241**, 13–17.
Tsien, R.W. & Tsien, R.Y. (1990) Calcium channels, stores, and oscillations. *Annu Rev Cell Biol* **6**, 715–760.
Tsien, R.W., Ellinor, P.T. & Horne, W.A. (1991) Molecular diversity of voltage-dependent Ca^{2+} channels. *Trends Pharmacol Sci* **12**, 349–354.
Tsujimoto, T., Jeromin, A., Saitoh, N., Roder, J.C. & Takahashi, T. (2002) Neuronal calcium sensor 1 and activity-dependent facilitation of P/Q-type calcium currents at presynaptic nerve terminals. *Science* **295**, 2276–2279.
Witcher, D.R., De Waard, M., Sakamoto, J., Franzini-Armstrong, C., Pragnell, M., Kahl, S.D. & Campbell, K.P. (1993) Subunit identification and reconstitution of the N-type Ca^{2+} channel complex purified from brain. *Science* **261**, 486–489.
Yue, Q., Jen, J.C., Nelson, S.F. & Baloh, R.W. (1997) Progressive ataxia due to a missense mutation in a calcium-channel gene. *Am J Hum Genet* **61**, 1078–1087.
Zhang, J.F., Randall, A.D., Ellinor, P.T., Horne, W.A., Sather, W.A., Tanabe, T., Schwarz, T.L. & Tsien, R.W. (1993) Distinctive pharmacology and kinetics of cloned neuronal Ca^{2+} channels and their possible counterparts in mammalian CNS neurons. *Neuropharmacology* **32**, 1075–1088.
Zwingman, T.A., Neumann, P.E., Noebels, J.L. & Herrup, K. (2001) Rocker is a new variant of the voltage-dependent calcium channel gene Cacna1a. *J Neurosci* **21**, 1169–1178.

Acknowledgments

We thank the Canadian Centre for Modeling Human Disease (www.cmhd.ca). This study was supported by grants-in-aid to J. C. R. from CIHR. J. G. S. was supported by the U.S. Department of Health and Human Services (NS41655). J. C. R. holds a Canada Research Chair. S. J. C. held a postdoctoral fellowship from the Royal Society of London. J. T. H. is the recipient of a NARSAD Young Investigator Award.